Available online at www.sciencedirect.com
ScienceDirect
Procedia Engineering 10 (2011) 518–523
Engineering Procedia

ICM11

Investigations into stress corrosion cracking behaviour of AZ91D magnesium alloy in physiological environment

Lokesh Choudhary[a*], Jeremy Szmerling[b], Robert Goldwasser[b], R.K. Singh Raman[a, b]
[a] Department of Mechanical and Aerospace Engineering, Monash University (Melbourne), VIC-3800, Australia
[b] Department of Chemical Engineering, Monash University (Melbourne), VIC-3800, Australia

Abstract

Mechanical integrity of biodegradable magnesium alloys implant remains an issue in bio-chemical and corrosive environment of human body because of their unacceptably high degradation rate. Therefore, understanding of simultaneous effect of stress and corrosive environment, i.e., stress corrosion cracking (SCC) of these alloys in physiological environment is essential before their actual use. To establish the SCC susceptibility, slow strain rate testing (SSRT) was carried out on the tensile specimens of a magnesium alloy, AZ91D in modified simulated body fluid (*m*-SBF) and air at different strain rates. Fracture surfaces of tested specimens were analysed using scanning electron microscopy (SEM) in order to examine the features of SCC. The alloy was found to be susceptible to SCC.

Selection and peer-review under responsibility of ICM11

Keywords: Magnesium; Stress corrosion cracking; Slow strain rate testing; Fractography; Physiological

1. Introduction

Titanium alloys and stainless steels have been widely used as body implants due to their excellent mechanical properties. However, the degradation products of these alloys may be toxic to the human body, and may cause long term adverse effects. Moreover, mechanical properties of these alloys differ vastly from those of human bone, which may cause stress shielding problem [1]. Furthermore, when these implants are used as temporary devices such as pins and screws, they remain as a foreign body to the human tissues even after the completion of healing process, and are commonly removed by a second surgery. The second surgical procedures not only increase the health care costs, but also increase the patient’s morbidity. Degradable biocompatible implants, which dissolve in physiological environment after a certain time of functional use, can be an appropriate solution. Thus, magnesium as a biodegradable implant material is an attractive candidate because they possess mechanical properties similar to those of human bone with significant biodegradability and biocompatibility [2]. However, in spite of the highly advantageous properties of magnesium and its alloys, they have found little application as body implants. The major limitation is the high corrosion rate of magnesium alloys in the physiological environment [2, 3]. As a result of corrosion-assisted degradation, magnesium alloys may lose their mechanical integrity in aggressive physiological environment before tissues have sufficient time to heal. Hence, before their

* Corresponding author. Tel.: +61 3 99051089
E-mail address: Lokesh.Choudhary@monash.edu

Selection and peer-review under responsibility of ICM11 doi:10.1016/j.proeng.2011.04.087

application as biodegradable implant, it will be essential to ensure the mechanical integrity of an alloy, at least until the temporary device (e.g., stents, pins and screws) has served its purpose.

An implant employed for the repair of a fractured bone must have sufficient strength to sustain and transmit the loading actions resulting from joints and muscular forces. The presence of mechanical loading along with corrosive physiological environment poses further complications, such as stress corrosion cracking (SCC), which is believed to be the most dangerous form of corrosion-assisted failures. SCC may be a particular concern for devices with sharp contours such as pins and screws that are used for securing orthopaedic implants. Stress corrosion cracks may propagate undetected to a sudden catastrophic failure. Such sudden failures caused by SCC of an implant may have serious consequences such as troublesome removal of failed device and painful irritation or inflammation of surrounding tissues. In the past, many instances of fracture due to stress corrosion cracking of metallic implants of stainless steels, titanium alloys and Co-Cr alloys have been reported [4, 5].

Magnesium alloys have also been reported to be susceptible to SCC in chloride environment [6-8]. However, there are only a few reports on SCC of magnesium alloys in physiological environment [9]. This study will investigate the SCC behaviour of AZ91D magnesium alloy in physiological environment using slow strain rate testing (SSRT) technique. SSRT experiments were performed at a range of strain rates followed by extensive fractography, in order to arrive at a robust conclusion on the SCC of a magnesium alloy in physiological environment.

2. Experimental

2.1. Materials and methods

Specimens were machined out of an as-cast AZ91D (Al: 8.8 wt%, Zn: 0.79 wt%, Mn: 0.21wt%) magnesium alloy billet. Typical dimension of round tensile SSRT specimen was 20mm (gauge length) and 3mm (gauge diameter). SSRT experiments were carried out in modified simulated body fluid (*m*-SBF) maintained at temperature 36.5 ± 0.5 ^{0}C using a water bath and a heater. The *m*-SBF solution is composed of 5.403 g/l NaCl, 0.504 g/l of $NaHCO_3$, 0.43 g/l of Na_2CO_3, 0.225 g/l of KCl, 0.23 g/l of $K_2HPO_4.3H_2O$, 0.31 g/l of $MgCl_2.6H_2O$, 100ml of 0.2M NaOH, 17.892 g/l of HEPES, 0.29 g/l of $CaCl_2$, 0.07 g/l of Na_2SO_4 and, 15ml of 1M NaOH. The *m*-SBF solution was buffered with 2-(4-(2-hydroxyethyl)-1-piperazinyl) ethanesulfonic acid (HEPES) at a physiological pH of 7.4 [10].

2.2. Slow strain rate testing (SSRT)

The SSRT experiments were carried out at a range of strain rates (1.2×10^{-7} to 4.3×10^{-7} s^{-1}) in *m*-SBF and air environments. In order to quantify the stress corrosion cracking susceptibility of AZ91D alloy in *m*-SBF, SCC susceptibility indices (I_{SCC}) were calculated for ultimate tensile strength (*UTS*) and time-to-failure (t_f). I_{SCC} was defined as a ratio of a given property in corrosive environment (*m*-SBF) and the corresponding value in an inert environment (air). A low I_{SCC} index corresponds to high SCC susceptibility, and when the I_{SCC} index approaches unity this means that there is no effect due to the test environment (i.e., the alloy is highly resistant to SCC in the particular test environment).

2.3. Fractography

To establish the intergranular and/or transgranular mode of SCC, fractography of the failed specimens was performed using scanning electron microscopy (SEM) after cleaning of corrosion products. Cleaning of fracture surfaces was performed using a solution of 20% CrO_3 and 10% $AgNO_3$.

3. Results and discussion

3.1. Slow strain rate testing

Stress *vs.* time plots for the tests conducted in *m*-SBF and air at different strain rates are presented in Fig. 1. It is evident from stress-time curves that the *UTS* and t_f were lower in *m*-SBF solution as compared to air at all the strain rates, which may be indicative of SCC. The values of *UTS* and t_f of specimens tested in *m*-SBF and air environments, as derived from SSRT experiments are shown in Table 1.

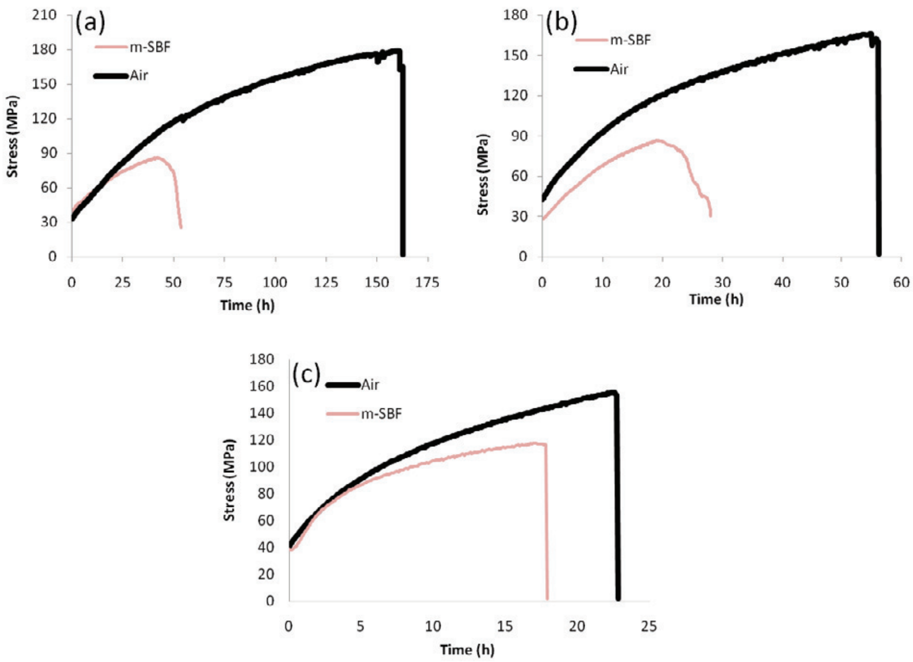

Fig. 1. Stress *vs.* time plots in *m*-SBF and air at different strain rates: (a) 1.2 x $10^{-7} s^{-1}$ (b) 2.2 x $10^{-7} s^{-1}$, *and (c)* 4.3 x $10^{-7} s^{-1}$

The SCC susceptibility indices for AZ91D obtained at different strain rates are presented in Fig. 2. At a strain rate of 1.2 × 10^{-7} s^{-1}, AZ91D showed highest SCC susceptibility in *m*-SBF. I_{SCC} approached to unity when strain rate was higher, i.e., 4.3 × 10^{-7} s^{-1}. Based on SCC susceptibility indices at all strain rates (Table 1), it can be deduced that AZ91D alloy suffered a significant SCC at lower strain rates, i.e., 1.2 × 10^{-7} s^{-1} and 2.2 × 10^{-7} s^{-1}, while alloy is significantly SCC resistant at higher strain rates i.e. 4.3 × 10^{-7} s^{-1}.

Table 1. Summary of SSRT results and calculated susceptibility indices at different strain rates

	UTS (MPa)			Time-to-failure (h)		
Strain rate (s^{-1})	*m*-SBF	Air	I_{SCC}	*m*-SBF	Air	I_{SCC}
1.2 × 10^{-7}	86.79	179.13	0.48	53.58	162.67	0.33
2.2 × 10^{-7}	86.34	166.35	0.52	28	56.25	0.49
4.3 × 10^{-7}	118.03	155.9	0.76	17.92	22.83	0.78

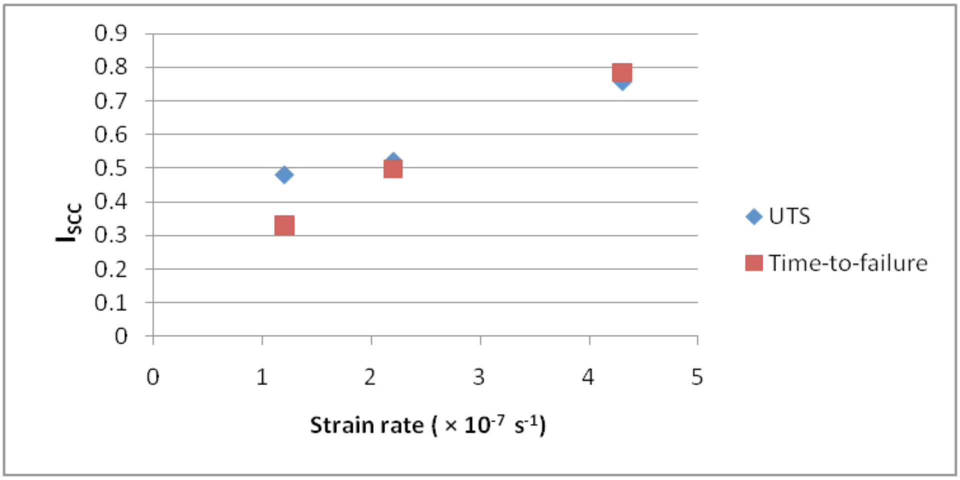

Fig. 2. Variation of SCC susceptibility indices (described both in terms of *UTS* and time-to-failure) with strain rate

3.2. Fractography

Typical fractographs of the AZ91D alloy tested in air are shown in Fig. 3. A higher magnification fractograph (Fig. 3b) revealed the dimple formation and also occasional feature of brittle fracture (the latter may be the fracture associated with secondary phase particles of the alloy (predominantly, β-phase)). These features of the air-tested specimens are consistent with those reported in the literature [6, 7].

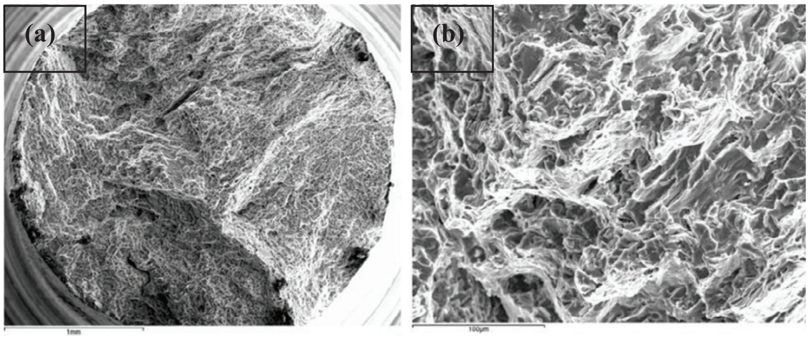

Fig. 3. Representative fractograph of all specimen tested in air: (a) overall fracture surface, and (b) evidence of ductile dimples

The fractographs for the specimens tested at strain rate 1.2 × 10^{-7} s^{-1} and 2.2 × 10^{-7} s^{-1} in *m*-SBF solution are shown in Fig. 4 and 5. The overall fracture surfaces show considerable amount of pitting along the circumference at both the strain rates (Fig. 4a and 5a). The higher magnification fractographs (Fig. 4b and 5b) reveal the distinctive features of SCC, i.e., transgranular cracking along with a few secondary cracks. The fractographs confirm that these alloys suffered a significant SCC, which is consistent with their low susceptibility indices at strain rates 1.2 × 10^{-7} s^{-1} and 2.2 × 10^{-7} s^{-1} (Table 1). However, the fractographs of the specimen tested in *m*-SBF at a higher strain rate, i.e., 4.3 × 10^{-7} s^{-1} (Fig. 6a and 6b) show the features similar to those of the specimens tested in air (Fig. 3a and 3b). On the basis of the fractographic features and their high susceptibility indices, it is suggested that specimen tested in *m*-SBF at strain rate 4.3 × 10^{-7} s^{-1} did not undergo SCC.

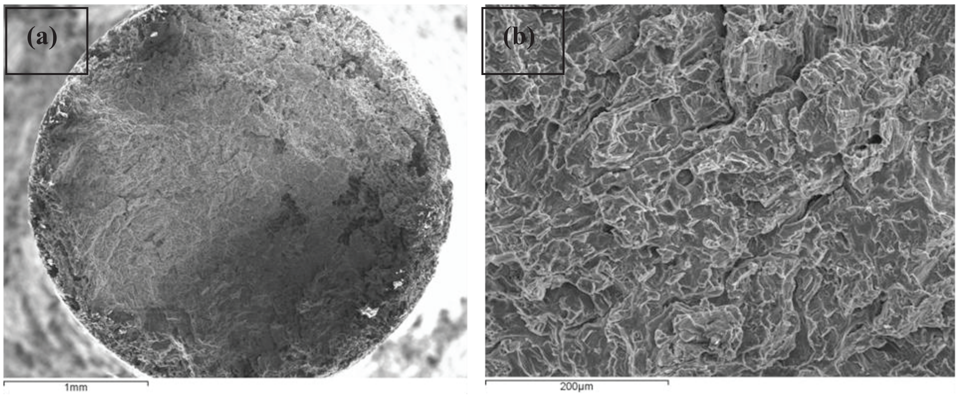

Fig. 4. Fractograph of specimen failed in *m*-SBF at strain rate 1.2×10^{-7} s^{-1}: (a) overall fracture surface of specimen, (b) fractograph showing tansgranular cacks and a few secondary cracks

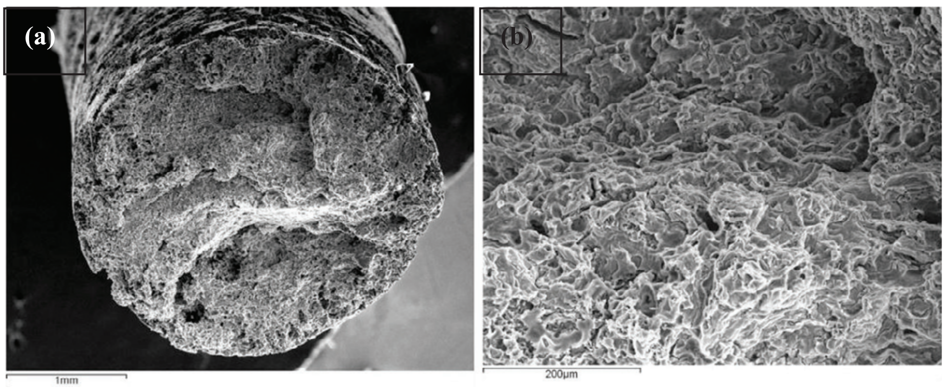

Fig. 5. Fractograph of specimen failed in *m*-SBF at strain rate 2.2×10^{-7} s^{-1}: (a) overall fracture surface of specimen, (b) evidence of trangranular cracking

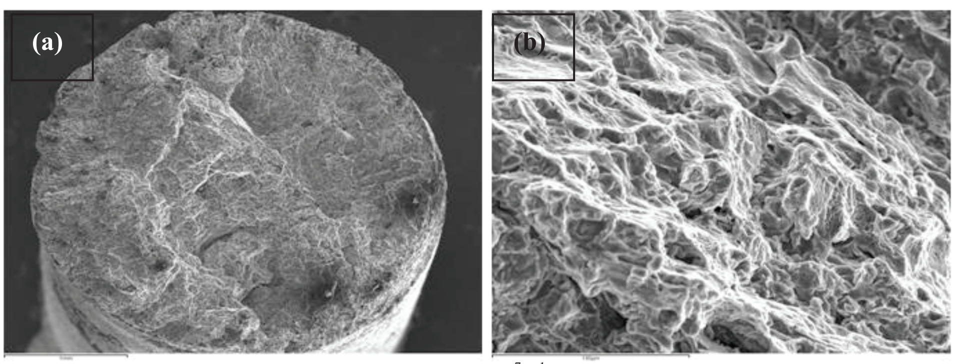

Fig. 6. Fractograph of specimen failed in *m*-SBF at strain rate 4.3×10^{-7} s^{-1}: (a) overall fracture surface of specimen, (b) fractograph revealing mechanical overload failure (ductile dimples)

Many authors reported [11, 12] that the stress-corrosion cracking of Mg-Al alloy is usually transgranular, but instances of intergranular cracking or mixture of both are also known. Transgranular

SCC of Mg is associated with conditions causing electrochemical breakdown or mechanical rupture of protective films at the crack surface, which allows hydrogen to enter the metal substrate. Furthermore, it is likely that the transgranular SCC in AZ91D alloy is consistent with mechanism involving hydrogen [13].

4. Conclusion

The main conclusions of this study are:

- AZ91D alloy is susceptible to SCC in *m*-SBF solution in the regime of low strain rates.
- Fractographic evidences showed mostly transgranular cracking along with a few localized secondary cracks.

Acknowledgements

The authors would like to acknowledge the support by Departments of Chemical Engineering and Mechanical & Aerospace Engineering, Monash University, Australia.

References

[1] Niinomi M. Recent metallic materials for biomedical applications. Metallurgical and Materials Transactions A 2002;33:477.

[2] Staiger MP, Pietak AM, Huadmai J, Dias G. Magnesium and its alloys as orthopedic biomaterials: A review. Biomaterials 2006;27:1728.

[3] Witte F, Fischer J, Nellesen J, Crostack H-A, Kaese V, Pisch A, Beckmann F, Windhagen H. In vitro and in vivo corrosion measurements of magnesium alloys. Biomaterials 2006;27:1013.

[4] Bombara G, Cavallini M. Stress corrosion cracking of bone implants. Corrosion Science 1977;17:77.

[5] Sivakumar M, Rajeswari S. Investigation of failures in stainless steel orthopaedic implant devices: pit-induced stress corrosion cracking. Journal of Materials Science Letters 1992;11:1039.

[6] Ben-Hamu G, Eliezer D, Dietzel W, Shin KS. Stress corrosion cracking of new Mg-Zn-Mn wrought alloys containing Si. Corrosion Science 2008;50:1505.

[7] Bobby Kannan M, Dietzel W, Blawert C, Atrens A, Lyon P. Stress corrosion cracking of rare-earth containing magnesium alloys ZE41, QE22 and Elektron 21 (EV31A) compared with AZ80. Materials Science and Engineering: A 2008;480:529.

[8] Ebtehaj K, Hardie D, Parkins RN. The influence of chloride-chromate solution composition on the stress corrosion cracking of a Mg-Al alloy. Corrosion Science 1988;28:811.

[9] Bobby Kannan M, Singh Raman RK. Evaluating the stress corrosion cracking susceptibility of Mg-Al-Zn alloy in modified-simulated body fluid for orthopaedic implant application. Scripta Materialia 2008;59:175.

[10] Oyane A, Kim HM, Furuya T, Kokubo T, Miyazaki T, Nakamura T. Preparation and assessment of revised simulated body fluids. Journal of Biomedical Materials Research Part A 2003;65A:188.

[11] Fairman L, Bray HJ. Transgranular see in Mg-Al alloys. Corrosion Science 1971;11:533.

[12] Stampella RS, Procter RPM, Ashworth V. Environmentally-induced cracking of magnesium. Corrosion Science 1984;24:325.

[13] Winzer N, Atrens A, Song G, Ghali E, Dietzel W, Kainer K, Hort N, Blawert C. A Critical Review of the Stress Corrosion Cracking (SCC) of Magnesium Alloys. Advanced Engineering Materials 2005;7:659.